HGG Advances

REPORT

CRISPR/Cas9-induced gene conversion between *ATAD3* paralogs

Shira Yanovsky-Dagan,[1] Ayala Frumkin,[1] James R. Lupski,[2,3,4] and Tamar Harel[1,5,*]

Abstract

Paralogs and pseudogenes are abundant within the human genome, and can mediate non-allelic homologous recombination (NAHR) or gene conversion events. The *ATAD3* locus contains three paralogs situated in tandem, and is therefore prone to NAHR-mediated deletions and duplications associated with severe neurological phenotypes. To study this locus further, we aimed to generate biallelic loss-of-function variants in *ATAD3A* by CRISPR/Cas9 genome editing. Unexpectedly, two of the generated clones underwent gene conversion, as evidenced by replacement of the targeted sequence of *ATAD3A* by a donor sequence from its paralog *ATAD3B*. We highlight the complexity of CRISPR/Cas9 design, end-product formation, and recombination repair mechanisms for CRISPR/Cas9 delivery as a nucleic acid molecular therapy when targeting genes that have paralogs or pseudogenes, and advocate meticulous evaluation of resultant clones in model organisms. In addition, we suggest that endogenous gene conversion may be used to repair missense variants in genes with paralogs or pseudogenes.

The human genome contains ~8,000 to 13,000 pseudogenes, depending on the annotation technology.[1–5] These include processed pseudogenes, derived from retrotransposition of processed mRNAs and thus lacking introns, and unprocessed pseudogenes, derived from segmental duplications also known as low-copy repeats. Processed pseudogenes are the most abundant type, presumably due to a burst of retrotranspositional activity in ancestral primates.[6–8]

Pseudogenes have long been considered nonfunctional, and the term paralog is sometimes used to describe genes that are transcribed and translated[1,5]; however, increasing evidence suggests that numerous pseudogenes have some form of biological activity. Gene-pseudogene interactions can occur at the DNA, RNA, or protein level. For example, at the DNA level, *CYP21A2P* causes adrenal hyperplasia by gene conversion with *CYP21A2*.[9] With regard to human genome rearrangements, glucocorticoid-remediable aldosteronism results from fusing the regulatory sequence from one paralog to another.[10] The most common trait observed in humans, red-green color blindness, is due to recombination between the red and green opsin gene paralogs *OPN1LW* and *OPN1MW*.[11] At the RNA level, *PTENP1* increases *PTEN* expression by sequestering microRNA and can act as a tumor suppressor.[12] At the protein level, *NOTCH2NL* genes activate NOTCH signaling by sequestering the inhibitory ligand DELTA, thus leading to expansion of the cortical progenitor population.[13,14]

Paralogs and pseudogenes can mediate non-allelic homologous recombination (NAHR). Three paralogs with extensive sequence homology are located in tandem at the *ATAD3* locus on chromosome 1p36.33: *ATAD3A, ATAD3B,* and *ATAD3C,* juxtaposed within an ~85 kb genomic interval (Figure 1A). This genomic architecture predisposes the region to genomic instability and reciprocal copy number variants (CNVs), deletions, and duplications. Biallelic deletions mediated by NAHR, most often spanning ~38 kb between *ATAD3B* and *ATAD3A* and less frequently ~67 kb between *ATAD3C* and *ATAD3A*, lead to an infantile-lethal presentation, including respiratory insufficiency, neonatal seizures, congenital contractures, corneal clouding and/or edema, pontocerebellar hypoplasia, and simplified sulcation and gyration.[15,16] Deletions between *ATAD3B* and *ATAD3A* lead to a fusion transcript under regulation of the weaker *ATAD3B* promoter, and thus show decreased expression of an ATAD3B/ATAD3A fusion protein that presumably is sufficient for fetal development but apparently cannot sustain life beyond the neonatal period.[17] The reciprocal, NAHR-mediated duplication at this locus, between *ATAD3C* and *ATAD3A,* results in a fusion gene encoding a dysfunctional protein.[18,19]

In order to pursue *in vitro* functional studies, we used CRISPR/Cas9 gene editing to engineer knockouts of *ATAD3A* in HEK293T cells, with a guide specific to *ATAD3A* that would not be expected to edit *ATAD3B* or *ATAD3C* (Figure S1). Transfected cells were seeded into wells at a very low dilution, with the aim of obtaining clonal populations by limiting dilution and clonal expansion. From among 38 wells that showed growth, we sequenced 19 wells. Fifteen of these had mixed populations of at least two sequences. Four wells were clonal: one showed a homozygous wild-type sequence indicating lack of editing or otherwise repair by homologous recombination; another had a single base pair insertion, as expected

[1]Department of Genetics, Hadassah Medical Organization, Jerusalem, Israel; [2]Department of Molecular and Human Genetics, Baylor College of Medicine, Houston, TX, USA; [3]Human Genome Sequencing Center, Baylor College of Medicine, Houston, TX, USA; [4]Texas Children's Hospital, Houston, TX, USA; [5]Faculty of Medicine, Hebrew University of Jerusalem, Jerusalem, Israel
*Correspondence: tamarhe@hadassah.org.il
https://doi.org/10.1016/j.xhgg.2022.100092.

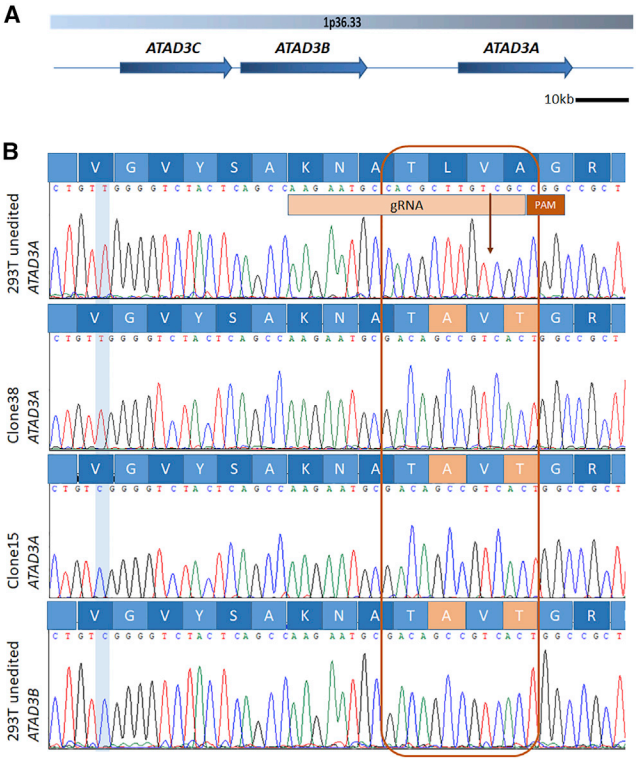

Figure 1. The *ATAD3* locus and sequences of the clones showing gene conversion. (A) The three paralogs of the *ATAD3* family (*ATAD3C, ATAD3B,* and *ATAD3A*) are situated in tandem, within an ~85 kb genomic interval on chromosome 1p36.33. Scale bar indicates 10kb. (B) Upper and lower panels show the sequence of wild-type *ATAD3A* and *ATAD3B* at the location targeted for editing (the gRNA sequence and protospacer adjacent motif (PAM) site [CGG] are indicated in the upper panel; arrow points to the cut site). Middle panels show the sequence of clones 38 and 15. The exchange of 13 bp by gene conversion is outlined within the magenta box. A single nucleotide upstream to this region (highlighted by a light blue box) is identical to *ATAD3A* in clone 38, and to *ATAD3B* in clone 15, indicating that the gene conversion event occurred independently in these two clones.

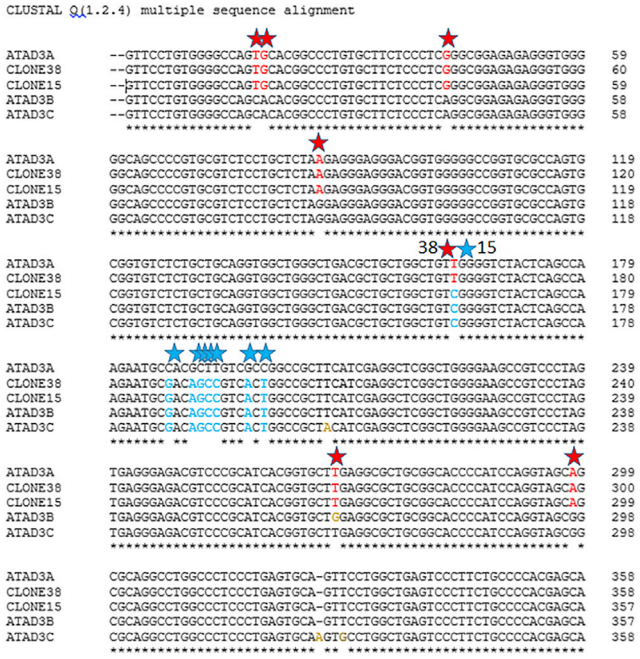

Figure 2. Multiple sequence alignment. The sequence of *ATAD3A* can be clearly recognized on either side of the gene conversion event. Red stars are unique to *ATAD3A;* blue stars are unique to *ATAD3B/3C*. Nucleotides in gold font are unique to either *ATAD3B* or *ATAD3C*.

to result from non-homologous end-joining repair (Figure S2). However, the other two clonal populations were unexpectedly found to have an in-frame 13 base pair (bp) sequence alteration at the cut site. This resulted in two missense variants: *ATAD3A* (RefSeq:NM_001170535.3): c.805_807delCTTinsGCC; p.(Leu269Ala) and c.811_813delGCCinsACT; p.(Ala271Thr), in addition to two synonymous variants that did not alter amino acids. Evaluation of the alteration revealed that a short sequence from either *ATAD3B* or *ATAD3C* had become embedded within *ATAD3A*, i.e., gene conversion (Figure 1B).

To ensure that the amplicon was amplified specifically from *ATAD3A,* and did not amplify *ATAD3B* or *ATAD3C,* we used two independent pairs of primers (Supplemental methods, Figure S1). We also sequenced *ATAD3B* and *ATAD3C* at the altered site in the HEK293T unedited cells, to verify that there were no single nucleotide polymorphisms (SNPs) at the *ATAD3B* or *ATAD3C* homologous loci (Figure S3). Based on a SNP 8 bp downstream of the conversion event, which is different in *ATAD3C,* we implicated *ATAD3B* rather than *ATAD3C* as the likely donor, although this origin cannot be proved for certain.

Multiple sequence alignment of the two "converted" clones (clone 15 and clone 38) as compared with the three *ATAD3* paralogs, indicated that the two clones had risen independently, as they differed at a position 24 bp upstream of the 13-bp conversion (Figure 2). The flanking regions of the 13-bp nucleotides are identical in the paralogs; therefore, it is not possible to determine the exact length of the conversion tract. For clone 38, the minimum of the donor tract is 13 bp and the maximum is 104 bp (calculated as the distance between the next upstream and downstream nucleotides that are unique to *ATAD3A* and not shared with *ATAD3B*). For clone 15, the minimum of the donor tract is 37 bp and the maximum is 181 bp (Figure 2). These ranges are consistent with the accepted mean length of 55 to 290 bp for conversion tracts.[20] Characterization of gene editing events by the Inference of CRISPR Edits (ICE) software, revealed that 14% to 25% of the population had been repaired by gene conversion (Figures 3 and S4). To check whether CRISPR/Cas9 had generated on-target deletions or duplications at the NAHR-prone *ATAD3* locus, we subjected the pool of edited cells to an Affymetrix CytoScan HD chromosomal microarray and compared the result with unedited HEK293T cells. No CNVs were observed (Figure S5).

CRISPR systems have significant therapeutic potential,[21] and much research is focused on minimizing off-target effects.[22] Reports of on-site unexpected effects are less

Figure 3. Relative percentages of edited populations. The relative contribution of each sequence to the initial population that underwent CRISPR/Cas9 editing was quantified by the ICE software (Synthego). Note that this software cannot differentiate between clones 15 and 38, such that 16% represents all clones that underwent gene conversion. Other estimates of the ICE software indicated gene conversion of 14% to 25% and are shown in Figure S4. The "N" in the upper sequence indicates a single nucleotide insertion, insT; the Sanger sequence is provided as Figure S2.

emphasized. "Bystander" deletions and duplications adjacent to the on-target cut site, complex rearrangements, and loss of the targeted chromosome have all been demonstrated; such events may escape detection by routine targeted genotyping assays.[23–26] In addition, unanticipated pseudogene-directed homology repair has been reported between *CD33* and its pseudogene *SIGLEC22P*. The authors emphasized the need for sequencing to detect CRISPR effects, rather than relying solely on changes in PCR fragment size, gene expression, or splicing patterns.[27]

Here, we show that CRISPR/Cas9 can lead to gene conversion, replacing a minimum of 13 nucleotides at the expected target site and resulting in two amino acid alterations in *ATAD3A*. The recognized pathogenic mutational spectrum at the *ATAD3* locus is largely driven by NAHR-mediated CNVs, generated by the DNA double-strand break repair (DSBR) pathway.[15,18,19] Gene conversion results from synthesis-dependent strand annealing[28] or from an alternate resolution of the double Holliday junctions by the error-prone break-induced replication (BIR) repair pathway, and may be mediated by template switches.[29] The migrating bubble-like replication fork results in conservative inheritance, with replacement of a short tract of the genome by a copy of the donor tract.[30,31] Half crossovers can form from interruption of BIR.[31] It is fathomable that gene conversion occurs at the *ATAD3A* locus, possibly introducing benign variation, such as multisite variants (MSVs) polymorphic across paralogous sequences and paralogous sequence variants.[32,33] The genomic distance between the *ATAD3* paralogs (total of ~85 kb) is within the cutoff of < 250 kb, which includes most known NAHR events, as has been empirically shown for *Alu-Alu* rearrangements.[34] In addition to CNVs, missense variants have been identified in *ATAD3A*, and it would be intriguing if these could be repaired by gene conversion from *ATAD3B* or *ATAD3C*.

Intentional NAHR or gene conversion between paralogs can have potential therapeutic benefit. CRISPR/Cas9-induced recombination between paralogs of the nucleotide-binding-site-leucine-rich-repeat (NBS-LRR) gene family in soybeans has been shown to accelerate disease resistance, by leading to novel chimeric paralogs with intact open reading frames.[35] In human cells, efficient gene conversion of *SMN2* to *SMN1* was shown to be induced by CRISPR/Cpf1 homology-directed repair and single-stranded oligodeoxynucleotides.[36] In addition, CRISPR/Cas9-induced gene conversion between *HBD* and *HBB*, encoding human hemoglobin subunits, has been documented; this correlated with *HBB* insertion and deletion rates, supporting gene conversion rather than PCR-mediated sequence shuffling between highly homologous sequences.[37,38] Indeed, spontaneous gene conversion between other paralogs of the β-globin cluster was the first instance of gene conversion recognized in the human genome.[39] CRISPR/Cas9 genome editing can also generate micronuclei and chromosome bridges initiating chromothripsis on the targeted chromosome.[40] Fascinatingly, McDermott et al.[41] reported a fortuitous cure of WHIM syndrome by chromothripsis, which resulted in deletion of the disease-causing gain-of-function allele.

Our report highlights the complexity of CRISPR/Cas9 design and recombinational repair mechanisms when considering both delivering nucleic acid therapeutics and when dealing with genes that have paralogs and pseudogenes. The specific mechanism of repair remains to be explored: whether the CRISPR/Cas9-generated event is repaired exclusively by a DSBR/homologous recombination mechanism (as shown in Figure S6), or whether it may also involve post-replication repair of one-ended, double-stranded DNA (oeDNA) generated at a collapsed fork,[42] the latter occurring through a BIR/microhomology-mediated BIR pathway that could result in a half-crossover or CNV.

These data also suggest experimental use of CRISPR/Cas9 in model organisms warrants meticulous evaluation of the resultant clones. On a complementary or reciprocal note, our findings foment interest that pathogenic variants in such genes may be repaired by mediating gene conversion intentionally. Further studies focused on the optimal characteristics of paralogs/pseudogenes for gene conversion are called for, to determine feasibility of such an approach. These include determining the optimal distance between paralogs/pseudogenes for CRISPR/Cas9-mediated gene conversion, whether specific sequence motifs enhance gene conversion rates, if intrachromosomal recombination events are preferred over interchromosomal events,[38] and if altering levels of proteins that mediate recombination[37] or introducing CRISPR/Cas9 editing at different

stages of the cell cycle[40] can influence gene conversion efficiency.

Data and code availability

The study did not generate datasets or code.

Supplemental information

Supplemental information can be found online at https://doi.org/10.1016/j.xhgg.2022.100092.

Acknowledgments

This research was supported by the Israel Science Foundation (grant no. 1663/17 to T.H.). Work in lab of J.R.L. is partially funded by US NINDS (R35 NS105078). We thank Dr. Ayal Hendel for technical consultation, Dr. Shamir Zenvirt for technical assistance, and Dr. Claudia Carvalho for insightful discussions.

Declaration of interests

J.R.L. has stock ownership in 23andMe, is a paid consultant for Regeneron Genetics Center, and is a co-inventor on multiple US and European patents related to molecular diagnostics for inherited neuropathies, eye diseases, and bacterial genomic fingerprinting. The Department of Molecular and Human Genetics at Baylor College of Medicine receives revenue from clinical genetic testing conducted at Baylor Genetics (BG) Laboratories. J.R.L. serves on the Scientific Advisory Board of BG.

Received: October 21, 2021
Accepted: January 19, 2022

References

1. Cheetham, S.W., Faulkner, G.J., and Dinger, M.E. (2020). Overcoming challenges and dogmas to understand the functions of pseudogenes. Nat. Rev. Genet. *21*, 191–201. https://doi.org/10.1038/s41576-019-0196-1.
2. Zhang, Z., Harrison, P.M., Liu, Y., and Gerstein, M. (2003). Millions of years of evolution preserved: a comprehensive catalog of the processed pseudogenes in the human genome. Genome Res. *13*, 2541–2558. https://doi.org/10.1101/gr.1429003.
3. Baertsch, R., Diekhans, M., Kent, W.J., Haussler, D., and Brosius, J. (2008). Retrocopy contributions to the evolution of the human genome. BMC Genomics *9*, 466. https://doi.org/10.1186/1471-2164-9-466.
4. Navarro, F.C., and Galante, P.A. (2013). RCPedia: a database of retrocopied genes. Bioinformatics *29*, 1235–1237. https://doi.org/10.1093/bioinformatics/btt104.
5. Pei, B., Sisu, C., Frankish, A., Howald, C., Habegger, L., Mu, X.J., Harte, R., Balasubramanian, S., Tanzer, A., Diekhans, M., et al. (2012). The GENCODE pseudogene resource. Genome Biol. *13*, R51. https://doi.org/10.1186/gb-2012-13-9-r51.
6. Torrents, D., Suyama, M., Zdobnov, E., and Bork, P. (2003). A genome-wide survey of human pseudogenes. Genome Res. *13*, 2559–2567. https://doi.org/10.1101/gr.1455503.
7. Zhang, Z., and Gerstein, M. (2004). Large-scale analysis of pseudogenes in the human genome. Curr. Opin. Genet. Dev. *14*, 328–335. https://doi.org/10.1016/j.gde.2004.06.003.
8. Balasubramanian, S., Zheng, D., Liu, Y.J., Fang, G., Frankish, A., Carriero, N., Robilotto, R., Cayting, P., and Gerstein, M. (2009). Comparative analysis of processed ribosomal protein pseudogenes in four mammalian genomes. Genome Biol. *10*, R2. https://doi.org/10.1186/gb-2009-10-1-r2.
9. Concolino, P., and Costella, A. (2018). Congenital adrenal hyperplasia (CAH) due to 21-hydroxylase deficiency: a comprehensive focus on 233 pathogenic variants of *CYP21A2* gene. Mol. Diagn. Ther. *22*, 261–280. https://doi.org/10.1007/s40291-018-0319-y.
10. Lifton, R.P., Dluhy, R.G., Powers, M., Rich, G.M., Cook, S., Ulick, S., and Lalouel, J.M. (1992). A chimaeric 11 beta-hydroxylase/aldosterone synthase gene causes glucocorticoid-remediable aldosteronism and human hypertension. Nature *355*, 262–265. https://doi.org/10.1038/355262a0.
11. Nathans, J., Thomas, D., and Hogness, D.S. (1986). Molecular genetics of human color vision: the genes encoding blue, green, and red pigments. Science *232*, 193–202. https://doi.org/10.1126/science.2937147.
12. Poliseno, L., Salmena, L., Zhang, J., Carver, B., Haveman, W.J., and Pandolfi, P.P. (2010). A coding-independent function of gene and pseudogene mRNAs regulates tumour biology. Nature *465*, 1033–1038. https://doi.org/10.1038/nature09144.
13. Suzuki, I.K., Gacquer, D., Van Heurck, R., Kumar, D., Wojno, M., Bilheu, A., et al. (2018). Human-specific *NOTCH2NL* genes expand cortical neurogenesis through delta/notch regulation. Cell *173*, 1370–1384.e16. https://doi.org/10.1016/j.cell.2018.03.067.
14. Fiddes, I.T., Lodewijk, G.A., Mooring, M., Bosworth, C.M., Ewing, A.D., Mantalas, G.L., et al. (2018). Human-specific *NOTCH2NL* genes affect notch signaling and cortical neurogenesis. Cell *173*, 1356–1369.e22. https://doi.org/10.1016/j.cell.2018.03.051.
15. Harel, T., Yoon, W.H., Garone, C., Gu, S., Coban-Akdemir, Z., Eldomery, M.K., et al. (2016). Recurrent de novo and biallelic variation of *ATAD3A*, encoding a mitochondrial membrane protein, results in distinct neurological syndromes. Am. J. Hum. Genet. *99*, 831–845. https://doi.org/10.1016/j.ajhg.2016.08.007.
16. Yap, Z.Y., Park, Y.H., Wortmann, S.B., Gunning, A.C., Ezer, S., Lee, S., Duraine, L., Wilichowski, E., Wilson, K., Mayr, J.A., et al. (2021). Functional interpretation of ATAD3A variants in neuro-mitochondrial phenotypes. Genome Med. *13*, 55. https://doi.org/10.1186/s13073-021-00873-3.
17. Desai, R., Frazier, A.E., Durigon, R., Patel, H., Jones, A.W., Dalla Rosa, I., et al. (2017). *ATAD3* gene cluster deletions cause cerebellar dysfunction associated with altered mitochondrial DNA and cholesterol metabolism. Brain *140*, 1595–1610. https://doi.org/10.1093/brain/awx094.
18. Gunning, A.C., Strucinska, K., Muñoz Oreja, M., Parrish, A., Caswell, R., Stals, K.L., Durigon, R., Durlacher-Betzer, K., Cunningham, M.H., Grochowski, C.M., et al. (2020). Recurrent de novo NAHR reciprocal duplications in the ATAD3 gene cluster cause a neurogenetic trait with perturbed cholesterol and mitochondrial metabolism. Am. J. Hum. Genet. *106*, 272–279. https://doi.org/10.1016/j.ajhg.2020.01.007.
19. Frazier, A.E., Compton, A.G., Kishita, Y., Hock, D.H., Welch, A.E., Amarasekera, S.S.C., Rius, R., Formosa, L.E., Imai-

Okazaki, A., Francis, D., et al. (2021). Fatal perinatal mitochondrial cardiac failure caused by recurrent. Med (N. Y.) *2*, 49–73. https://doi.org/10.1016/j.medj.2020.06.004.
20. Jeffreys, A.J., and May, C.A. (2004). Intense and highly localized gene conversion activity in human meiotic crossover hot spots. Nat. Genet. *36*, 151–156. https://doi.org/10.1038/ng1287.
21. Ma, H., Marti-Gutierrez, N., Park, S.W., Wu, J., Lee, Y., Suzuki, K., Koski, A., Ji, D., Hayama, T., Ahmed, R., et al. (2017). Correction of a pathogenic gene mutation in human embryos. Nature *548*, 413–419. https://doi.org/10.1038/nature23305.
22. Aquino-Jarquin, G. (2021). Current advances in overcoming obstacles of CRISPR/Cas9 off-target genome editing. Mol. Genet. Metab. *134*, 77–86. https://doi.org/10.1016/j.ymgme.2021.08.002.
23. Simeonov, D.R., Brandt, A.J., Chan, A.Y., Cortez, J.T., Li, Z., Woo, J.M., Lee, Y., Carvalho, C.M.B., Indart, A.C., Roth, T.L., et al. (2019). A large CRISPR-induced bystander mutation causes immune dysregulation. Commun. Biol. *2*, 70. https://doi.org/10.1038/s42003-019-0321-x.
24. Kosicki, M., Tomberg, K., and Bradley, A. (2018). Repair of double-strand breaks induced by CRISPR-Cas9 leads to large deletions and complex rearrangements. Nat. Biotechnol. *36*, 765–771. https://doi.org/10.1038/nbt.4192.
25. Shin, H.Y., Wang, C., Lee, H.K., Yoo, K.H., Zeng, X., Kuhns, T., Yang, C.M., Mohr, T., Liu, C., and Hennighausen, L. (2017). CRISPR/Cas9 targeting events cause complex deletions and insertions at 17 sites in the mouse genome. Nat. Commun. *8*, 15464. https://doi.org/10.1038/ncomms15464.
26. Alanis-Lobato, G., Zohren, J., McCarthy, A., Fogarty, N.M.E., Kubikova, N., Hardman, E., Greco, M., Wells, D., Turner, J.M.A., and Niakan, K.K. (2021). Frequent loss of heterozygosity in CRISPR-Cas9-edited early human embryos. Proc. Natl. Acad. Sci. U S A *118*. e2004832117. https://doi.org/10.1073/pnas.2004832117.
27. Shaw, B.C., and Estus, S. (2021). Pseudogene-mediated gene conversion after CRISPR-Cas9 editing demonstrated by partial. CRISPR J. *4*, 699–709. https://doi.org/10.1089/crispr.2021.0052.
28. Hastings, P.J. (2010). Mechanisms of ectopic gene conversion. Genes (Basel) *1*, 427–439. https://doi.org/10.3390/genes1030427.
29. Mayle, R., Campbell, I.M., Beck, C.R., Yu, Y., Wilson, M., Shaw, C.A., Bjergbaek, L., Lupski, J.R., and Ira, G. (2015). DNA REPAIR. Mus81 and converging forks limit the mutagenicity of replication fork breakage. Science *349*, 742–747. https://doi.org/10.1126/science.aaa8391.
30. Parks, M.M., Lawrence, C.E., and Raphael, B.J. (2015). Detecting non-allelic homologous recombination from high-throughput sequencing data. Genome Biol. *16*, 72. https://doi.org/10.1186/s13059-015-0633-1.
31. Saini, N., Ramakrishnan, S., Elango, R., Ayyar, S., Zhang, Y., Deem, A., Ira, G., Haber, J.E., Lobachev, K.S., and Malkova, A. (2013). Migrating bubble during break-induced replication drives conservative DNA synthesis. Nature *502*, 389–392. https://doi.org/10.1038/nature12584.
32. Lindsay, S.J., Khajavi, M., Lupski, J.R., and Hurles, M.E. (2006). A chromosomal rearrangement hotspot can be identified from population genetic variation and is coincident with a hotspot for allelic recombination. Am. J. Hum. Genet. *79*, 890–902. https://doi.org/10.1086/508709.
33. Campbell, I.M., Gambin, T., Jhangiani, S., Grove, M.L., Veeraraghavan, N., Muzny, D.M., Shaw, C.A., Gibbs, R.A., Boerwinkle, E., Yu, F., and Lupski, J.R. (2016). Multiallelic positions in the human genome: challenges for genetic analyses. Hum. Mutat. *37*, 231–234. https://doi.org/10.1002/humu.22944.
34. Song, X., Beck, C.R., Du, R., Campbell, I.M., Coban-Akdemir, Z., Gu, S., Breman, A.M., Stankiewicz, P., Ira, G., Shaw, C.A., and Lupski, J.R. (2018). Predicting human genes susceptible to genomic instability associated with. Genome Res. *28*, 1228–1242. https://doi.org/10.1101/gr.229401.117.
35. Nagy, E.D., Stevens, J.L., Yu, N., Hubmeier, C.S., LaFaver, N., Gillespie, M., Gardunia, B., Cheng, Q., Johnson, S., Vaughn, A.L., et al. (2021). Novel disease resistance gene paralogs created by CRISPR/Cas9 in soy. Plant Cell Rep. *40*, 1047–1058. https://doi.org/10.1007/s00299-021-02678-5.
36. Zhou, M., Hu, Z., Qiu, L., Zhou, T., Feng, M., Hu, Q., et al. (2018). Seamless genetic conversion of *SMN2* to *SMN1* via CRISPR/Cpf1 and single-stranded oligodeoxynucleotides in spinal muscular atrophy patient-specific induced pluripotent stem cells. Hum. Gene Ther. *29*, 1252–1263. https://doi.org/10.1089/hum.2017.255.
37. Javidi-Parsijani, P., Lyu, P., Makani, V., Sarhan, W.M., Yoo, K.W., El-Korashi, L., Atala, A., and Lu, B. (2020). CRISPR/Cas9 increases mitotic gene conversion in human cells. Gene Ther. *27*, 281–296. https://doi.org/10.1038/s41434-020-0126-z.
38. Burgio, G. (2020). Gene conversion following CRISPR/Cas9 DNA cleavage: an overlooked effect. Gene Ther. *27*, 245–246. https://doi.org/10.1038/s41434-020-0154-8.
39. Slightom, J.L., Blechl, A.E., and Smithies, O. (1980). Human fetal G gamma- and A gamma-globin genes: complete nucleotide sequences suggest that DNA can be exchanged between these duplicated genes. Cell *21*, 627–638. https://doi.org/10.1016/0092-8674(80)90426-2.
40. Leibowitz, M.L., Papathanasiou, S., Doerfler, P.A., Blaine, L.J., Sun, L., Yao, Y., Zhang, C.Z., Weiss, M.J., and Pellman, D. (2021). Chromothripsis as an on-target consequence of CRISPR-Cas9 genome editing. Nat. Genet. *53*, 895–905. https://doi.org/10.1038/s41588-021-00838-7.
41. McDermott, D.H., Gao, J.L., Liu, Q., Siwicki, M., Martens, C., Jacobs, P., Velez, D., Yim, E., Bryke, C.R., Hsu, N., et al. (2015). Chromothriptic cure of WHIM syndrome. Cell *160*, 686–699. https://doi.org/10.1016/j.cell.2015.01.014.
42. Lupski, J.R. (2021). Clan genomics: from OMIM phenotypic traits to genes and biology. Am. J. Med. Genet. A *185*, 3294–3313. https://doi.org/10.1002/ajmg.a.62434.